Western Australian School of Mines

Exploration Geophysics

Full waveform inversion of time-lapse VSP data

Anton Egorov

This thesis is presented for the Degree of
Doctor of Philosophy
of
Curtin University

August 2018

Contents

Summary 3

Introduction 4

Chapter 1 Current state of time-lapse Vertical Seismic Profile 5

Chapter 2 Time-lapse FWI strategies and the preprocessing workflow 6

Chapter 3 FWI of VSP datasets acquired with geophones 12

Chapter 4 FWI of VSP datasets acquired with DAS 15

Chapter 5 A perspective of permanent monitoring using FWI of VSP data 19

Conclusions 23

Acknowledgments 24

References 25

Summary

Time-lapse vertical seismic profiling (VSP) is one of the technologies for monitoring of hydrocarbon production and CO_2 geosequestration. This methodology has become more attractive in recent years due to the introduction of distributed acoustic sensing (DAS), which uses fiber optic cables instead of more traditional geophones as seismic receivers. Despite these technological advances, using traditional quantitative interpretation methods of time-lapse VSP data is challenging due to the irregular distribution of source-receiver offsets, which is not an issue for surface seismic where these methods are used. One way to overcome this challenge is to use full waveform inversion (FWI), which does not require regular offsets. I present a workflow of elastic FWI applied to offset vertical seismic profile data for the purpose of identification and estimation of time-lapse changes. Application of this workflow to both synthetic and field geophone VSP data shows that elastic FWI is able to detect and quantify the time-lapse anomaly in P wave velocity with the magnitude of 100–150 m/s introduced by the injection of CO_2.

Standard FWI algorithms are developed for use on data corresponding to particle velocity, often measured along the three dimensions. DAS, however, measures a single quantity, which is an approximation of the strain or strain rate along the fiber. Thus, the application of these methods to DAS data requires conversion of DAS data to particle velocity along the fiber. I present a filter that converts DAS VSP data into an estimate of particle velocity along the fiber. Field measurements show that the conversion result is close to vertical particle velocity as measured by geophones. I apply the earlier proposed FWI workflow to a multioffset DAS data set acquired at the CO2CRC Otway Project site in Victoria, Australia. FWI reveals salient subhorizontal layering consistent with the known geology of the site. Tests on synthetic data show that DAS can be used together with permanent sources for permanent monitoring using FWI. Tests also show that the results of such monitoring can potentially be improved using alternative FWI strategies.

Introduction

Time-lapse seismic is an established technology for monitoring hydrocarbon production and CO_2 sequestration. Onshore seismic monitoring is mostly conducted using surface 3-D seismic surveys, which are sometimes complemented with offset/walkaway/3-D vertical seismic profile (VSP) surveys (Daley et al., 2008). VSP has a number of advantages over surface seismic, as the receivers are placed closer to the target and the level of noise on VSP data is significantly lower. However, quantitative interpretation (QI) of VSP data by established methods, such as amplitude-variation-with-offset (AVO) inversion, is challenging, due to irregular offset distribution. One way to overcome this challenge is to apply full waveform inversion (FWI), which does not require regular illumination of the target. Furthermore, VSP data have certain properties that make it particularly suitable for FWI. VSP gathers are generally low noise and contain no surface waves, which are difficult to model and may not be repeatable due to variations of near-surface properties. Also, the presence of strong transmitted waves on VSP data provides a reliable starting tomographic model and a constraint on velocity changes, so that the data can be successfully inverted without very low frequencies (Neklyudov et al., 2013).

The objective of this work is to create a 2D FWI workflow that is capable of detecting localized changes in the subsurface, such as a small amount of injected CO_2, using VSP data. In recent years, the VSP method is receiving more attention due to the introduction of Distributed Acoustic Sensing (DAS) (Parker et al., 2014) – a novel acquisition technology, which allows one to use fibre-optic cables as seismic receivers suitable for VSP. Relatively low price and the suitability for permanent installation makes DAS a promising solution for monitoring, so this FWI workflow needs to be applicable to DAS VSP data, as well as to traditional geophone VSP data.

This document is a short abstract of the thesis that I prepared to complete the joint PhD program between Lomonosov Moscow State University and Curtin University. This abstract contains the main results of the research conducted during the PhD and uses the text and figures from the published papers and abstracts. The thesis is in the Russian language.

Chapter 1 Current state of time-lapse Vertical Seismic Profile

VSP is a seismic exploration method that involves placing the seismic receivers in a well, while the sources remain on/near the surface of the Earth. Originally, the idea of measuring the seismic wavefield in wells was expressed in a patent by Fessenden (1917). Seismic datasets acquired with VSP geometry had been used since then (Levin and Lynn, 1958), but the method only acquired its English name and gained popularity after the translation of the "Vertical Seismic Profiling" textbook into English by Galperin and White (1974).

Today, in most cases, traditional seismic imaging methods are applied to VSP data, such as Kirchhoff migration (Dillon, 1990) and more modern reverse-time migration (Shi and Wang, 2016). QI of VSP data is rarely performed. If QI is performed, it is, in most cases, a modification of AVO used to determine the properties of the reservoir (Leaney et al., 1999). The application of traditional QI methods to VSP is complicated due to the uneven illumination of the target.

Recent years showed a rise of interest towards FWI of VSP data as an alternative to the existing QI methods. There are a number of published examples of successful elastic FWI applications to VSP (Charara et al., 1996, Owusu et al., 2016). However, there are very few cases of FWI of VSP data being used for seismic monitoring. In one example, Liang et al. (2013) were able to quantify the changes in the medium introduced by the steam injection in a heavy oil field using acoustic FWI. Yang et al. (2014), however, were unable to detect the time-lapse difference in velocities introduced by the CO_2 injection using FWI, which was partly attributed to the survey geometry (the receivers were placed above the target, which was therefore illuminated only by reflected waves).

To this day, there are no published examples of QI of VSP data acquired with DAS sensors. Several successful applications of DAS VSP as a tool for subsurface imaging have been reported, particularly for reservoir monitoring (Mateeva et al., 2014).

Chapter 2 Time-lapse FWI strategies and the preprocessing workflow

For the time-lapse inversion of the field VSP data, a strategy needs to be chosen and the field data preprocessing flow needs to be developed. These two problems are explored in the separate sections of this chapter. This chapter contains material from a paper submitted to the Geophysical Prospecting journal, but not yet published.

2.1. Comparison of different strategies for time-lapse full waveform inversion

Full waveform inversion (Virieux and Operto, 2009) involves finding the minimum of an objective function that measures misfit between measured and modelled data:

$$\min C(\mathbf{m}) \tag{2.1}$$

The goal of FWI lies in finding a model of the subsurface that explains the observed data. The objective function acts as a measure of similarity between the observed and modelled datasets. In most cases, the least-squares objective function is used:

$$C(\mathbf{m}) = \frac{1}{2}\sum_{s}(\Delta\mathbf{d}^{*}\Delta\mathbf{d}), \tag{2.2}$$

where **m** is the model vector, **Δd** is the data misfit vector, i.e. the difference between the observed and modelled datasets, s denotes summation over all sources and * is conjugate transpose. Here, for simplicity, no weighting is applied to the misfit between the modelled and field data.

In traditional FWI, minimization is performed using local iterative gradient-based techniques, the gradient is obtained using the adjoint-state method (Plessix, 2006). For optimization, steepest descent, conjugate gradient, L-BFGS, Gauss-Newton or Truncated Newton methods can be applied. Forward problem can be solved using finite-difference or finite-element methods.

A few approaches exist for the estimation of time-lapse changes using FWI. In most cases, the inversion of baseline and monitor datasets is being conducted separately and sequentially. The difference between the baseline and monitor inversion results is considered to be the time-lapse difference. The result of baseline inversion is almost always taken as the initial model for the monitor inversion. The inversion of the monitor dataset is sometimes modified by introducing an alternative misfit, such as double-difference (Denli and Huang, 2009):

$$\tilde{\Delta \mathbf{d}} = (\mathbf{d}^{\mathbf{M}}_{\mathbf{obs}} - \mathbf{d}^{\mathbf{B}}_{\mathbf{obs}}) - (\mathbf{d}^{\mathbf{M}}_{\mathbf{syn}} - \mathbf{d}^{\mathbf{B}}_{\mathbf{syn}}) \tag{2.3}$$

Here B and M denote baseline and monitor datasets respectively. The advantage of the double-difference strategy is that it prevents the inaccuracy of the baseline model from influencing the time-lapse image. Sometimes, the changes introduced by FWI are restricted to a certain localized region (Asnaashari et al., 2015), which is called "target-oriented" or "localized" FWI. In this thesis, I perform sequential inversion of baseline and monitor datasets. The monitor data is inverted both with the traditional least-squares misfit and with the double-difference misfit. There are also examples of joint inversion of baseline and monitor data (Maharramov et al., 2016), but these methods are currently out of scope of our research.

To assist FWI in computing the time-lapse image, I suggest using constrained optimization methods for the monitor inversion, such as L-BFGS-B (Byrd et al., 1995). Constrained optimization imposes box constraints on the solution of the problem (2.1), which can be expressed as follows:

$$\mathbf{l} \leq \mathbf{m} \leq \mathbf{u} \tag{2.4}$$

Depending on the a priori sign of parameter change, the baseline inversion result is set as a lower or upper L-BFGS-B bound for the monitor inversion. If the baseline inversion result is set as a lower bound, the monitor inversion is not allowed to decrease the parameter. If the baseline inversion result acts as an upper bound, the monitor inversion is not allowed to increase the parameter.

To determine the amplitude and direction of changes in subsurface properties, accurate analysis of the expected time-lapse response is usually performed before conducting the field seismic survey (Caspari et al., 2015). However, such analysis is not required for the presented method. In this study, only the general knowledge about the sign of the changes of elastic parameters acts as prior information.

Below, a comparison of the discussed methods is displayed using a simple horizontally-layered model. The inverted frequency band is 8-36 Hz, multiscale approach is applied for the inversion (Bunks et al., 1995). Baseline inversion results are shown in Figure 2.1. To model the time-lapse response, I place a 30 m thick CO_2 plume at ~1100 m depth. The small thickness of the plume together with rather narrow frequency band allows me to display the advantages of the bound constrained time-lapse inversion. The differences in the subsurface properties introduced by the CO_2 plume are as follows: dV_P=-200 m/s, dV_S=35 m/s, $d\rho$=-80 kg/m^3.

The monitor inversion results are compared to the true differences in properties in Figure 2.2. The sequential inversion results shown in the second column are contaminated by the time-lapse noise, which is caused by the inaccuracies of the baseline model. If the double-difference objective function is used, the events that were not explained by the baseline inversion are removed from the misfit, which makes the double-difference monitor inversion (Figure 2.2, third column) less sensitive to the inaccuracy of the baseline model (Asnaashari et al., 2015).

In both the sequential and double-difference results, dV_P is underestimated, $d\rho$ is overestimated and dV_S is slightly overestimated. All around the main image of the plume, secondary maxima/minima with the opposite sign of time-lapse changes can be seen. Application of the bound constrained inversion (Figure 2.2, fourth column) helps to get rid of these secondary maxima/minima in the time-lapse image.

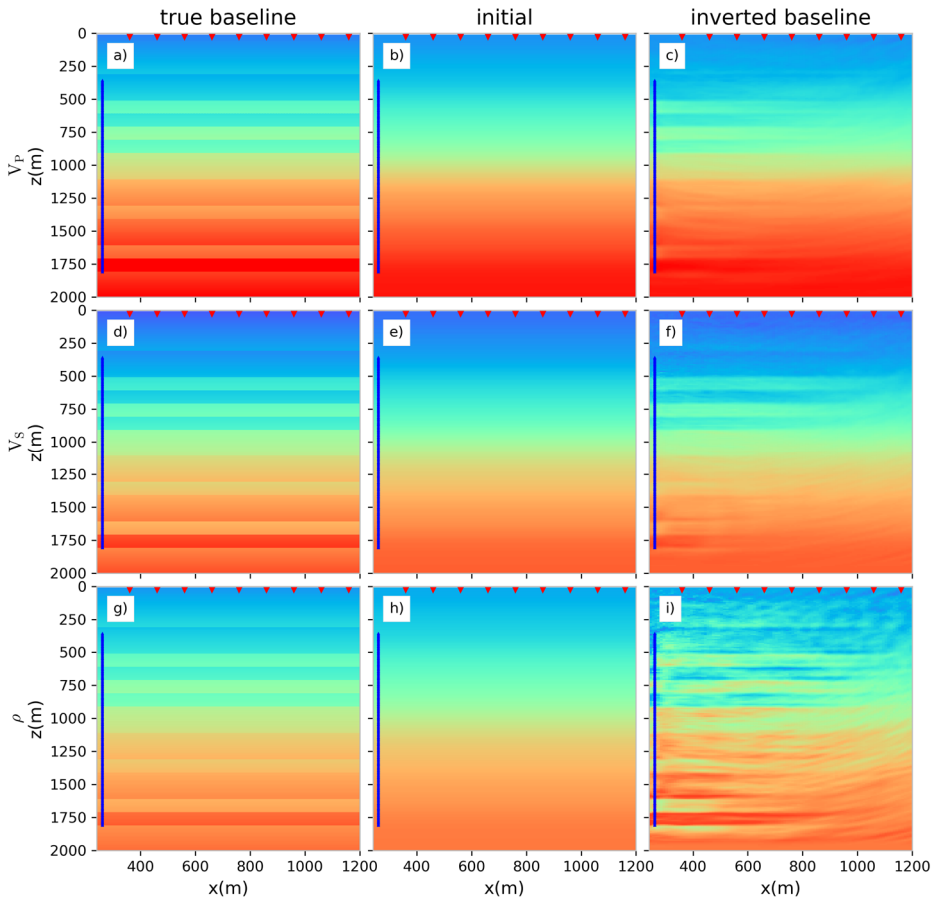

Figure 2.1. Baseline inversion result. V_P (a-c), V_S (d-f) and density (g-i) models: true (a, d ,g); initial (b, e, h) and inverted (c, f, i). Walkaway VSP geometry is used, sources and receivers are displayed.

This study shows that sequential inversion with conventional L_2 misfit is feasible only when the misfit of the baseline inversion is small relative to the time-lapse difference (i.e. baseline inversion is accurate). Double-difference and bound-

constrained double-difference strategies can improve the inversion results significantly.

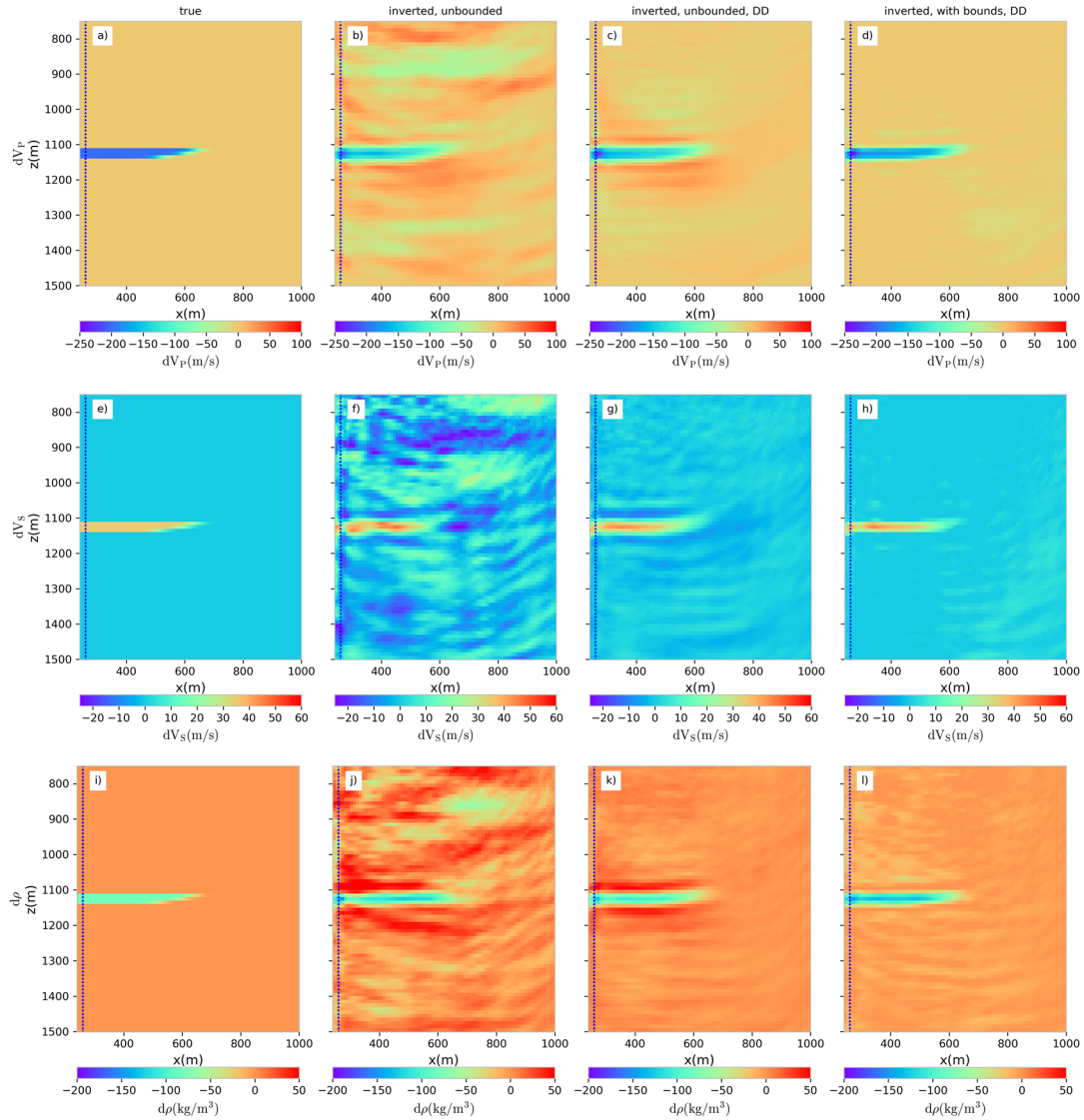

Figure 2.2. True difference in subsurface properties compared to time-lapse inversion results. VP (a-d), VS (e-h) and density (i-j): true differences (a, e, i); sequential FWI results (b, f, j); double-difference FWI results (c, g, k); double-difference FWI results with bounds (d, h, l).

2.2. Preprocessing of time-lapse VSP for time-lapse full waveform inversion

This section contains the preprocessing flow that I developed specifically for the purposes of the time lapse VSP FWI, which looks as follows:

1) Correlation
2) Orientation of horizontal components
3) QC
4) Noise removal
5) Regularization
6) Converting the zero-phase vibroseis data to minimum-phase
7) Wavelet estimation
8) Deconvolution (optional)

9) Conventional processing steps: setting maximum inversion time, resampling, top muting
10) Conversion to 2D amplitudes
11) Data windowing for the inversion
12) Quality control of the starting model

Most of the procedures in the workflow are conventional for VSP processing. Here, we focus only on the stages of the workflow that are unconventional or particularly important.

The quality control of the data is critical for successful application of FWI. Bad traces, if not removed, introduce noise into the misfit gather (Figure 2.3), which may influence the reconstructed models.

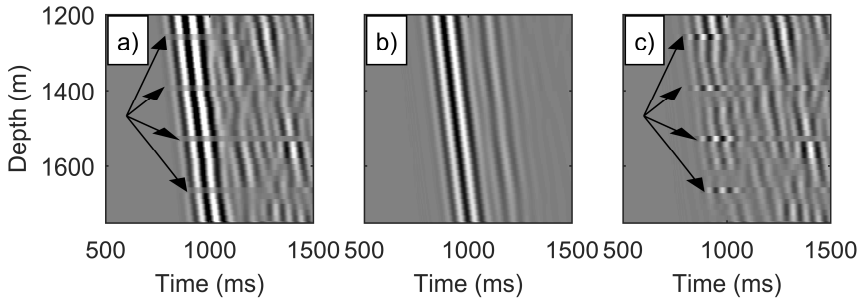

Figure 2.3. Field gather with bad traces (a), synthetic gather at the first iteration (b) and their misfit (c). The highest amplitudes in the misfit occur at the locations of bad traces. These high values of misfit will deteriorate the inversion results unless the traces are removed.

The deconvolution, though it is the only optional step in the flow, helps to highlight and control the time-lapse changes in the data (Figure 2.4).

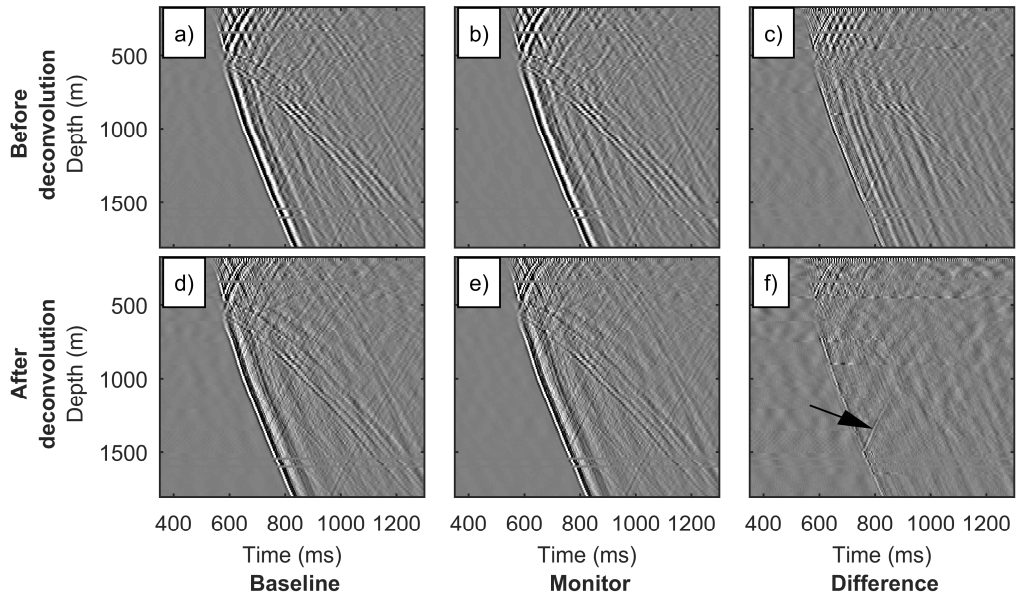

Figure 2.4. Field VSP gathers (vertical component) for baseline (a, d) and monitor (b, e) surveys and their difference (c, f) before (a-c) and after (d-f) deconvolution. The arrow on the difference between gathers after deconvolution shows a reflection from the CO_2 plume.

The inverted field data has 3D geometrical spreading, while 2D FWI involves 2D wave propagation with 2D geometrical spreading. I apply the conversion strategy described by Pica et al. (1990) due to its simplicity and suitability for VSP geometry.

At the first iteration (which means on the lowest frequency of the low-pass filter in the multiscale approach), one can check the quality of the V_P and V_S starting models by comparing (and overlaying) both components of the preprocessed field gathers and the synthetic gathers calculated in the starting model. If the gathers were preprocessed correctly and the signal was estimated correctly, the wavelet shapes of the direct P wave on the synthetic and field gathers will be identical. If there is little to no cycle skipping (e.g. Figure 2.5, where the cycle skipping does not occur in both P- and S- waves apart from the direct S-wave on shallow receivers), then the starting models are good enough.

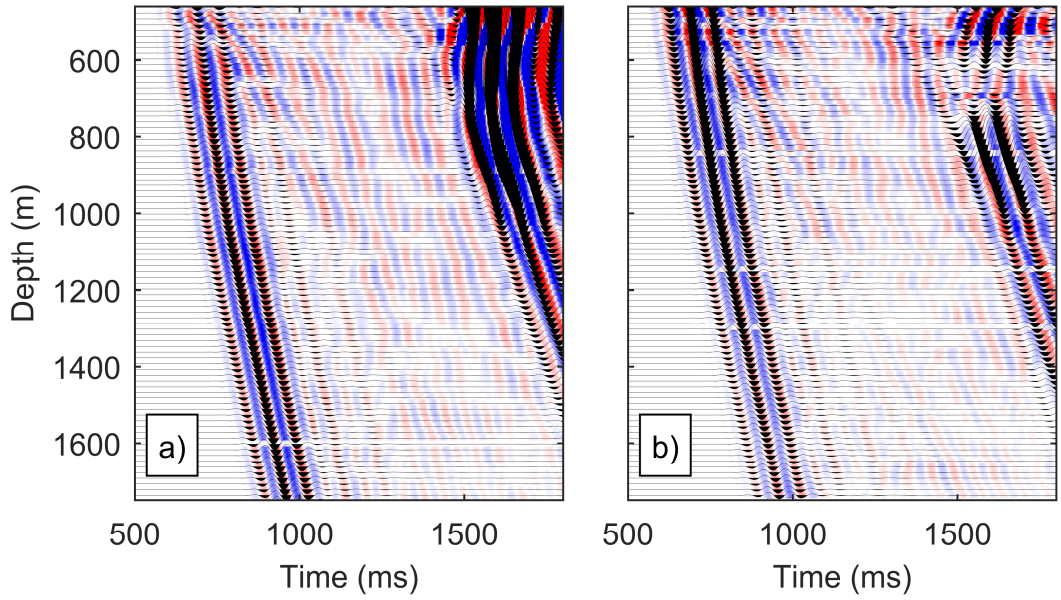

Figure 2.5. The quality control of starting models for the vertical (a) and horizontal (b) components. Field gathers are shown in color, synthetic gathers are shown as traces. Almost no cycle skipping is observed for the direct waves. The red in the field data almost always corresponds to the black wiggles in synthetics (within half a period).

Chapter 3 FWI of VSP datasets acquired with geophones

The following chapter is based on the paper by Egorov et al. (2017) and the abstract by Egorov et al. (2018b). It borrows figures and text from both the paper and the abstract.

We conduct time-lapse FWI of synthetic and field VSP datasets in order to acquire an image of the time-lapse changes introduced by the CO_2 injection. Only offset VSP geometries are considered due to the fact that they record direct waves, which facilitate the FWI workflow (Neklyudov et al., 2013). Seismic receivers are placed both above and below the CO_2 plume.

Synthetic datasets were computed using a model of the Otway site in Victoria, Australia (Glubokovskikh et al., 2016, Caspari et al., 2015). Field time-lapse VSP datasets we invert were acquired during Stage 2C of the Otway project. Stage 2C of the Otway project involved an injection of 15,000 tons of CO2/CH4 gas mixture into a saline aquifer at ~1500 m depth. Offset VSP, walkaway VSP and 3D VSP surveys were acquired. Here, we use only offset VSP data. There are four offset VSP shot points on the site. Six surveys were conducted – a baseline and five monitors. For this study, we use a baseline dataset and a dataset from the monitor survey acquired directly after the end of 15,000 t injection.

We conduct elastic time-domain FWI implemented in an open-source inversion package (Köhn, 2011, Köhn et al., 2012). We first update the baseline velocity model using the baseline dataset. In order to mitigate the nonlinearity of the inverse problem, the multiscale approach by Bunks et al. (1995) is applied, that is, the baseline inversion is carried out from low to high frequencies by applying high-cut Butterworth filters to the inverted data. The high-cut filter slope for the first iteration is placed at 12 Hz frequency. When the misfit change between two consequent iterations is small enough, the slope is progressively shifted to 80 Hz in steps of 1 Hz. To obtain the time-lapse image, sequential strategy is used, i.e. baseline inversion result is taken as input to the monitor inversion. As the misfit of the baseline inversion is small, inversion strategies with the conventional L2 misfit and double-difference misfit produce similar results, so the results for the conventional L2 misfit are shown.

In Figure 3.1, baseline inversion results for single-offset VSP geometry are displayed. The synthetic data being inverted was generated using a 2D finite-difference code. In Figure 3.2, time-lapse image of the difference in V_P obtained by the inversion

is compared to the true V_P difference between the baseline and monitor models. Sources and receivers are displayed on the models. Maximum receiver depth is 1800 m.

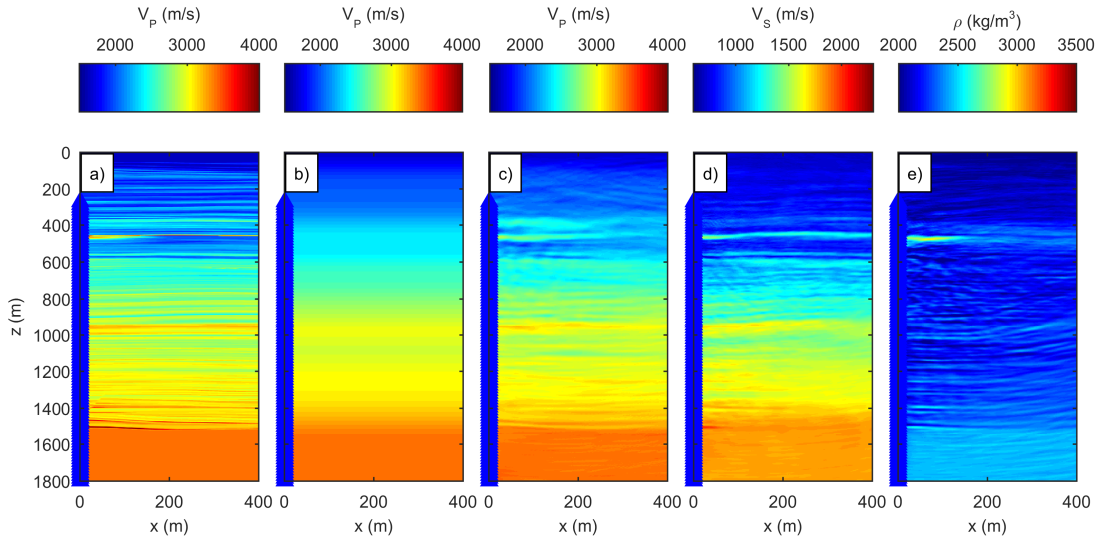

Figure 3.1. Single-offset VSP baseline inversion results: true V_P model (a), initial V_P model (b), inverted V_P model (c), inverted V_S model (d), inverted density model (e).

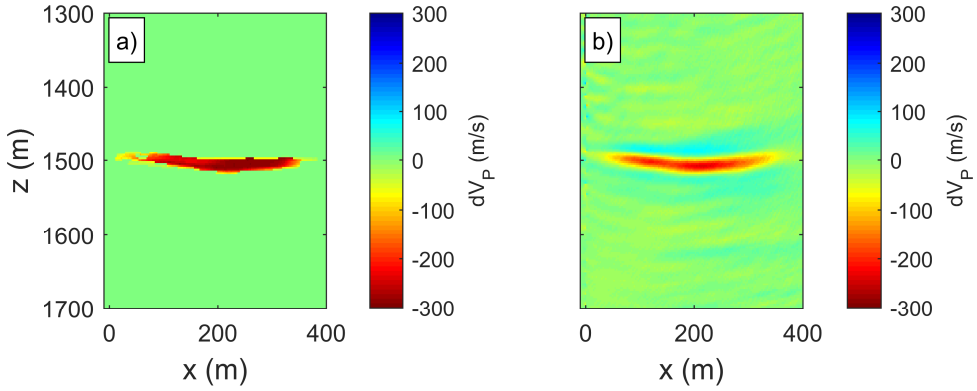

Figure 3.2. Single -offset VSP time-lapse inversion results: true change in V_P (a), inverted change in V_P (b).

In Figure 3.3, we show the FWI result obtained by inverting a baseline field single-offset VSP dataset (offset 1035 m) from Stage 2C of the Otway Project. In Figure 3.4, we compare the time-lapse images of the CO2 plume obtained by the FWI of shot points 1 (offset 825 m), 2 (offset 1035 m) and 3 (offset 1082 m). The quality of the inversion result for shot point 3 is lower due to lower repeatability of seismic data for this shot point. Still, all three images produced by FWI are easier to interpret than the result of conventional processing of time-lapse VSP data (Figure 3.5).

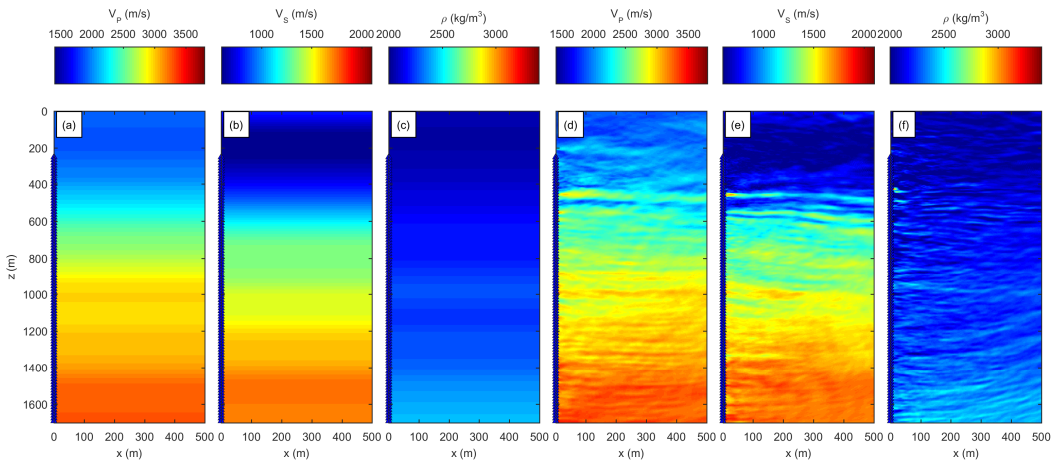

Figure 3.3. Field single-offset VSP baseline inversion results: initial V_P model (a), initial V_S model (b), initial density model (c), inverted V_P model (d), inverted V_S model (e), inverted density model (f).

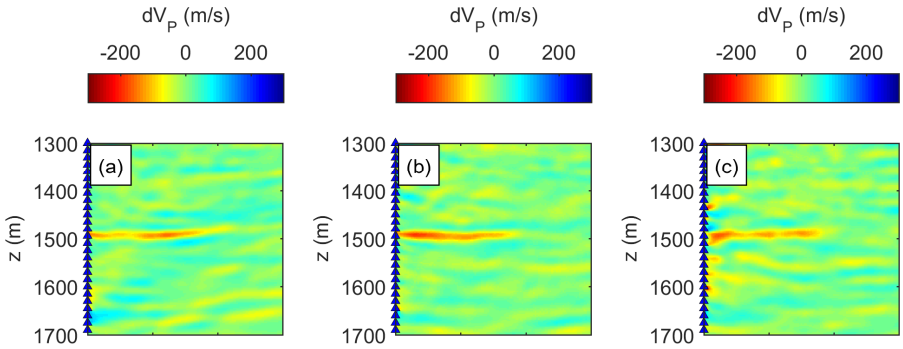

Figure 3.4. Field single-offset VSP time-lapse inversion results. Images of CO_2 plume identified by the inversion of VSP data from different shot points: shot point 1 (a), shot point 2 (b) and shot point 3 (c).

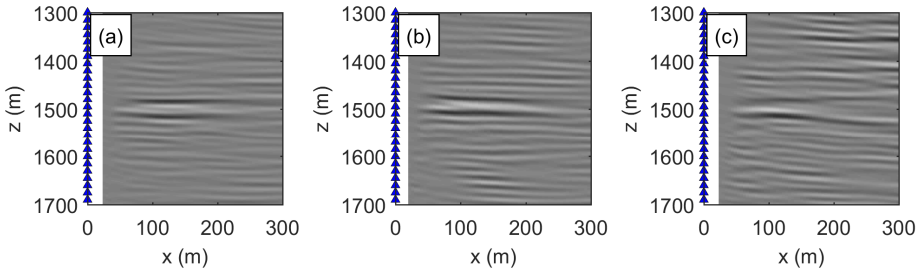

Figure 3.5. Field single-offset VSP time-lapse processing results. Images of CO_2 plume identified by conventional processing of time-lapse VSP data from different shot points: shot point 1 (a), shot point 2 (b) and shot point 3 (c).

Chapter 4 FWI of VSP datasets acquired with DAS

The following chapter is based on the paper by Egorov et al. (2018c) and borrows figures and text from the paper.

Distributed acoustic sensing (DAS) is a novel field acquisition solution, a technology that enables recording of seismic data using fibre-optic cables instead of traditional receivers such as geophones and hydrophones. Since permanent installation of DAS cable is possible, it can be conveniently used for reservoir monitoring. In most published studies DAS VSP data are analysed using conventional VSP imaging techniques. Our objective is to apply elastic 2D FWI to a field onshore VSP dataset acquired with a DAS recording system and a seismic vibrator source. Existing FWI methodologies use input pressure or particle velocity recordings, and hence cannot be directly applied to DAS measurements. While a new inversion technology may be developed that will directly use the strain measurements supplied by DAS (Podgornova et al., 2017), we opt for converting DAS recordings to vertical component of particle velocity instead.

DAS systems measure strain or strain rate, a temporal derivative of strain (Parker et al., 2014). Figure 4.1 shows a schematic diagram of a DAS measurement.

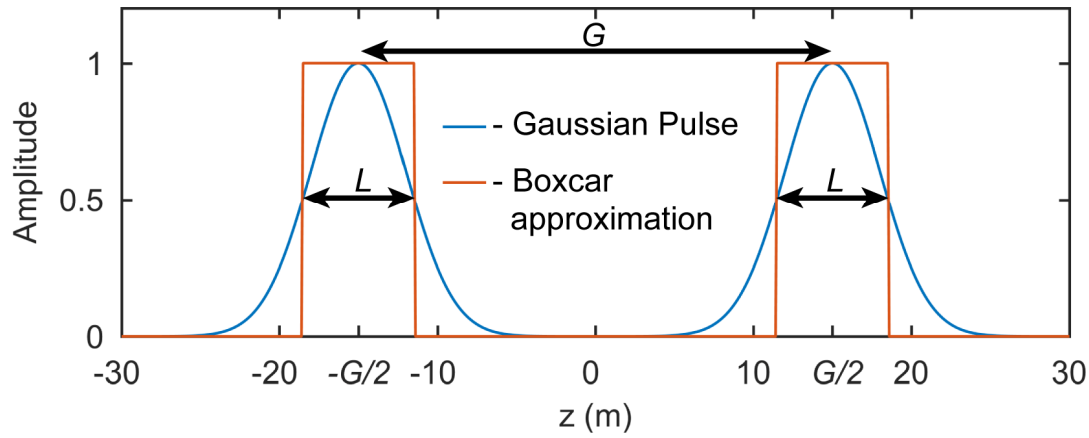

Figure 4.1. Schematic of DAS measurement. G is the gauge length, L is the pulse width.

We come up with a conversion filter that transforms the DAS response into particle velocity:

$$F_{REG}(k_z) = \frac{ik_z}{4\sin(k_z L/2)\sin(k_z G/2)}, \tag{4.1}$$

z axis follows the fiber and k_z is the vertical component of the wavenumber. The filter is to be applied after the Fourier transform along the fiber. As the filter might have

zero values in the denominator, it is convenient to regularize it as follows (Hatton et al., 1986):

$$F_{REG}(k_z) = \frac{ik_z}{4\sin(k_z L/2)\sin(k_z G/2) + \gamma}. \quad (4.2)$$

Or, if in the given wavenumber band at least one of the sine functions in the denominator has negative values, as follows:

$$F_{REG}(k_z) = \frac{ik_z \sin(k_z L/2)\sin(k_z G/2)}{4\sin^2(k_z L/2)\sin^2(k_z G/2) + \gamma}. \quad (4.3)$$

An example of such a conversion applied to a DAS seismic gather acquired in the field for different values of γ is presented in Figure 4.2. A geophone gather is shown as a reference. It can be seen that quite an accurate conversion is possible. Only the events with near-infinite apparent velocity are not reconstructed (green rectangle), which remains the only limitation of the proposed algorithm. This limitation is related to the fundamental physical constraints of DAS systems. Choosing the regularization coefficient is subjective. The process of choosing this parameter is outlined by (Correa et al., 2017). It involves starting with a very small γ (almost unregularized) and increasing it gradually.

After DAS gathers are converted to the vertical component of particle velocity, they can be inverted with the traditional least-squares FWI (Virieux and Operto, 2009, Köhn et al., 2012). Our FWI workflow is similar to the workflow we use for the inversion of geophone VSP data (Egorov et al., 2017). We apply conventional elastic FWI to the converted data excluding the source-generated S-wave from the field data inversion (Figure 4.3). In the field data, these waves lack high frequencies, possibly due to complex wave propagation in the near-field of the source. Not including this wave into the inversion leads to poor quality of recovered S-wave velocity and density models. However, the workflow still provides a realistic estimate of P-wave velocity. The P-wave velocity model estimated by FWI of field VSP dataset acquired with DAS recording system contains salient subhorizontal layering, which matches with other data available for the site. The match between the recovered P-wave velocity model and the P-wave velocity log is affected by the fact that this FWI workflow is not constrained by the log data, but it is still reasonable in most parts of the available log.

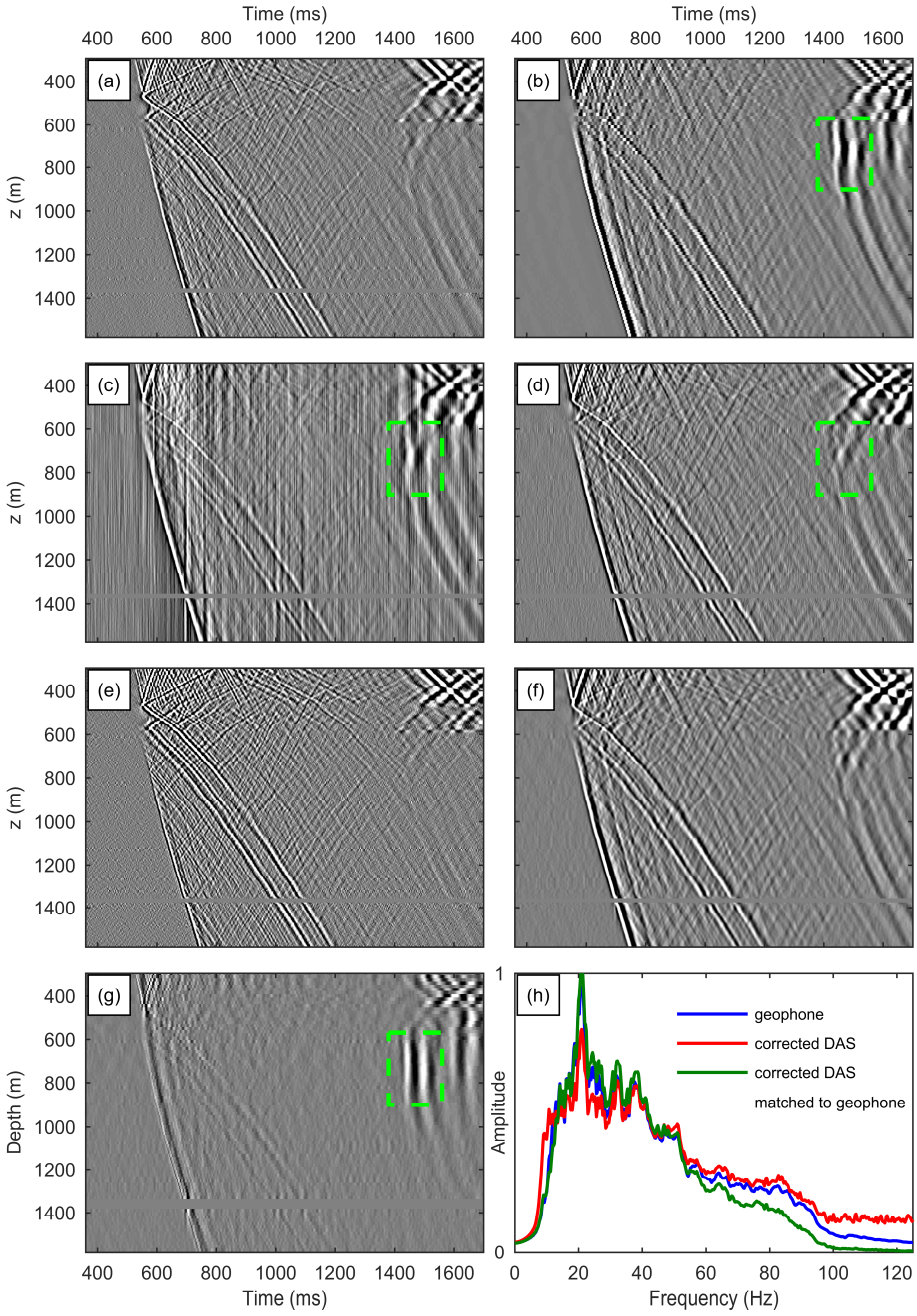

Figure 4.2. Comparison of DAS and vertical geophone gathers. Raw DAS gather (a); vertical geophone gather (b); DAS gather after conversion with $\gamma = 0$ (c), $\gamma = 0.0005$ (d), $\gamma = 0.05$ (e); DAS gather after conversion with $\gamma = 0.0005$ matched to geophone gather using a Wiener filter (f); difference between the geophone gather 4b and corrected matched DAS gather 4f decimated to geophone trace interval (g); and comparison of average amplitude spectra of gathers displayed in subplots 4b, 4d and 4f (h). The green box outlines an S-wave event which is not correctly recovered by the regularized conversion due to its low k_z value.

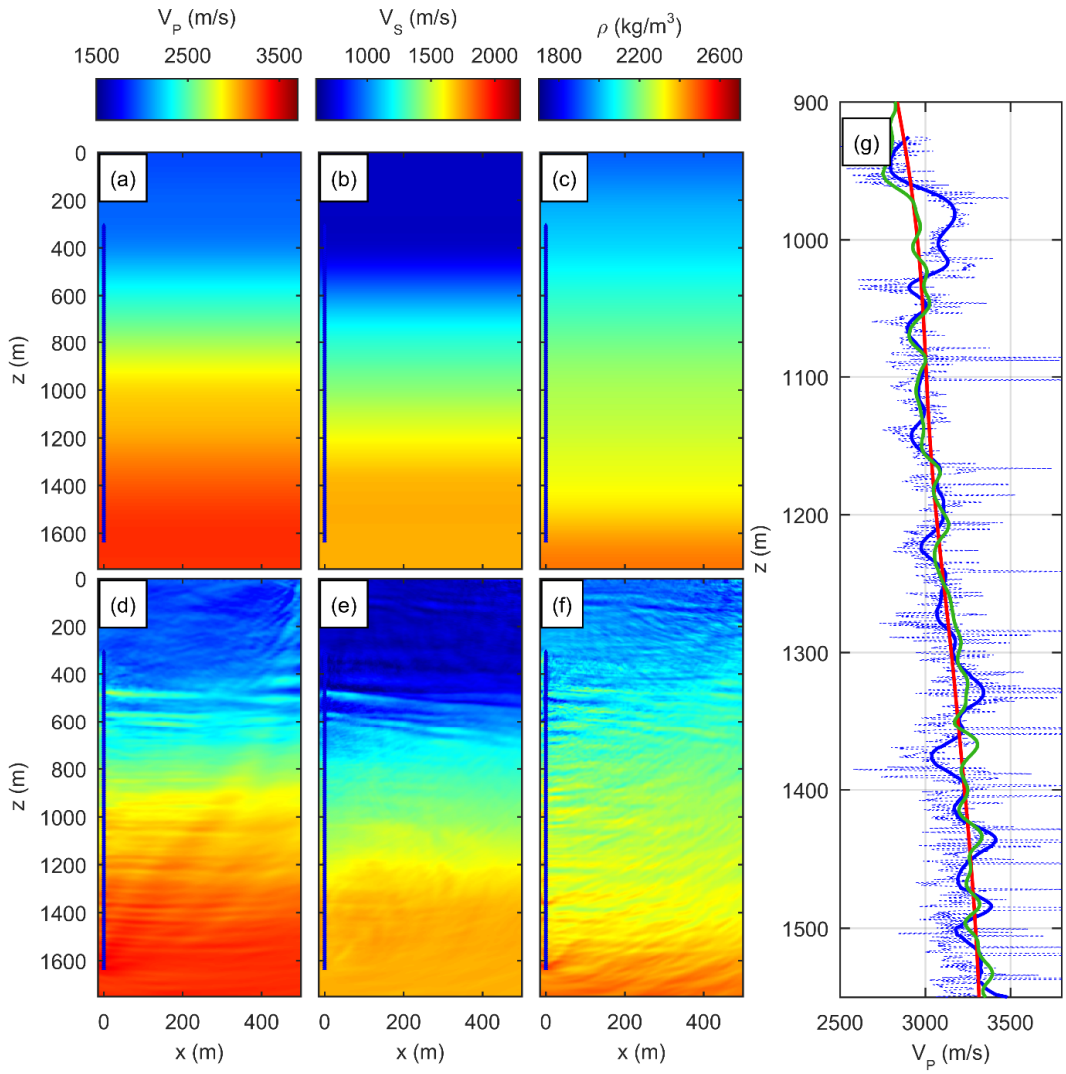

Figure 4.3. Inversion of field data. Initial (a-c) and inverted (d-f) V_P (a, d), V_S (b,e), and density (c,f) models of the subsurface and a comparison of inverted V_P model 5 m away from the well with the available log data (g). In (g), V_P log is a dashed blue line, V_P log smoothed to approximate resolution of the inversion is a solid blue line, V_P starting model is shown in red and the V_P inverted model is shown in green. Receiver locations are overlayed on the models.

Here, we are only interpreting the P-wave velocity model obtained from our measurements. The improvement of S-wave velocity and density models will be the subject of our future work. Reliable estimation of S-velocity is essential for making quantitative interpretation of VSP data.

Our study shows that FWI of DAS VSP data is feasible. As DAS is often used for reservoir monitoring, the presented workflow can be applied to build the baseline model of the subsurface.

Chapter 5 A perspective of permanent monitoring using FWI of VSP data

The following chapter is based on the abstract by (Egorov et al., 2018a). It borrows figures and text from the abstract.

In surface seismic/Vertical Seismic Profile (VSP) monitoring projects, the quick turnaround time is one of the key components. It is important to make quick decisions based on the image of the changes in the subsurface. Consequently, acquisition and processing of seismic data needs to be as fast as possible. Currently, it is conventional to conduct monitoring surveys once in a few months with data processing, in case of an established workflow, taking a few days or weeks. While such acquisition and processing speed is often sufficient, it can be further improved using permanent source and receiver installation. DAS sensors (Parker et al., 2014) can be cemented behind the well's casing and used as permanent receivers. For permanently deployed sources, several options were developed recently (Dou et al., 2017, Kasahara et al., 2013).

During the upcoming Stage 3 of the Otway project (Jenkins et al., 2017) it is planned to conduct monitoring of the CO_2 injection using a number of permanent sources and DAS systems. Here, we perform a feasibility study of such monitoring using 2D elastic FWI on two synthetic datasets. We suggest building baseline models of seismic properties using a multi-offset VSP survey potentially acquired with conventional vibroseis sources. After that, we aim to obtain the time-lapse image of the changes in the subsurface using a sparse subset of permanent sources (2 or 3 in our synthetic examples). In order to facilitate the time-lapse inversion, we apply double-difference and localized inversion strategies introduced in Chapter 2.

We apply conventional elastic time-domain FWI based on L_2 norm and multiscale approach with V_P-V_S-density parameterization (Köhn, 2011, Köhn et al., 2012). We model and invert the vertical component of particle velocity gathers acquired with a vertical force source. In real life, the vertical component of particle velocity can be obtained by applying a conversion filter to the field DAS data. Such a conversion filter is introduced in Chapter 4 of this dissertation.

We use the model displayed in Figure 5.1 to demonstrate the usability of different time-lapse FWI strategies for permanent monitoring. Figure 5.1 shows the true initial and inverted models for the baseline inversion.

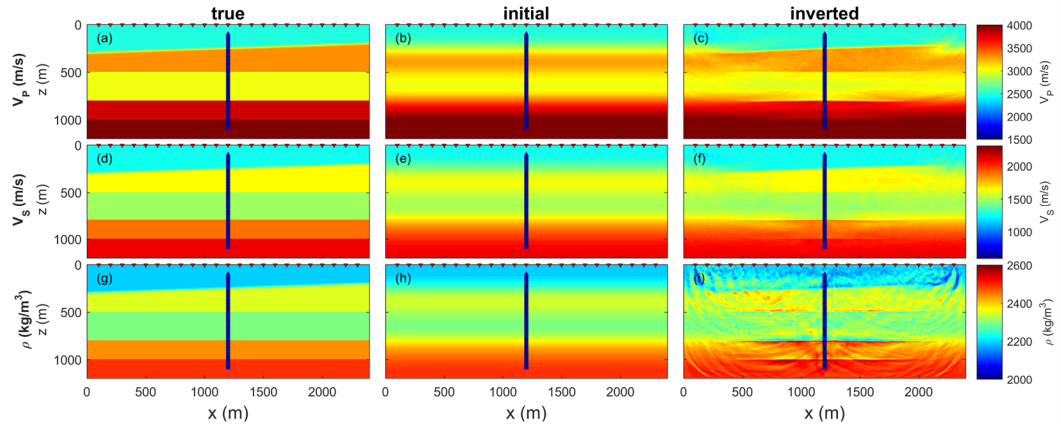

Figure 5.1. Baseline FWI results. V_P (a-c), V_S (d-f) and density (g-i) models: true (a, d, g), initial (b, e, h) and inverted (c, f, i).

To mimic CO_2 sequestration conditions, the changes in V_P and density were introduced in the monitor model. The comparison of time-lapse V_P anomalies identified by different inversion strategies is shown in Figure 5.2. Sequential FWI strategy produces a smeared image of the anomaly in case of 3 sources (Figure 5.2c). Introducing a priori information by localizing the search in the layer from 450 to 700 m assists the inversion significantly (Figure 5.2d), and the double-difference inversion helps to produce a clearer image (Figure 5.2e).

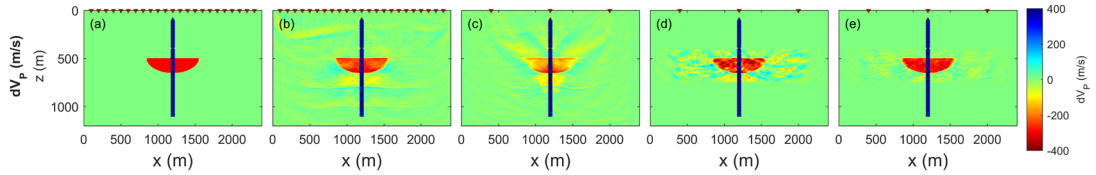

Figure 5.2. True time-lapse anomaly in V_P (a) compared to the anomalies identified by different FWI strategies: sequential with all sources (b), sequential with 3 permanent sources (c), target-oriented sequential with 3 permanent sources (d), target-oriented double-difference with 3 permanent sources (e). Maximum frequency is 80 Hz.

The workflow is further validated using a realistic 3D full-earth model of the Otway site that was created using the available log and field seismic data (Glubokovskikh et al., 2016). A monitor model for the planned Stage 3 injection was obtained using fluid flow simulations. We extract a vertical slice of the baseline and monitor models that passes through the DAS-equipped CRC-3 well and the planned location of two permanent sources to create a 2D model. Using this model, we calculate synthetic VSP gathers. For this particular feasibility study, we only perform a monitor inversion using the true baseline model as the initial model. In Figure 5.3, we compare the true VP difference and the images of the CO2 plume that can be obtained using 16 sources (with ~50 m interval from -35 to 740 m) and two permanent

sources (15 m and 615 m offsets). Target-oriented inversion strategy is used in both cases (inversion takes place in a layer with depths from 1425 to 1650 m). It can be seen that the images of the time-lapse anomaly are comparable, the permanent-source image has slightly smaller amplitude.

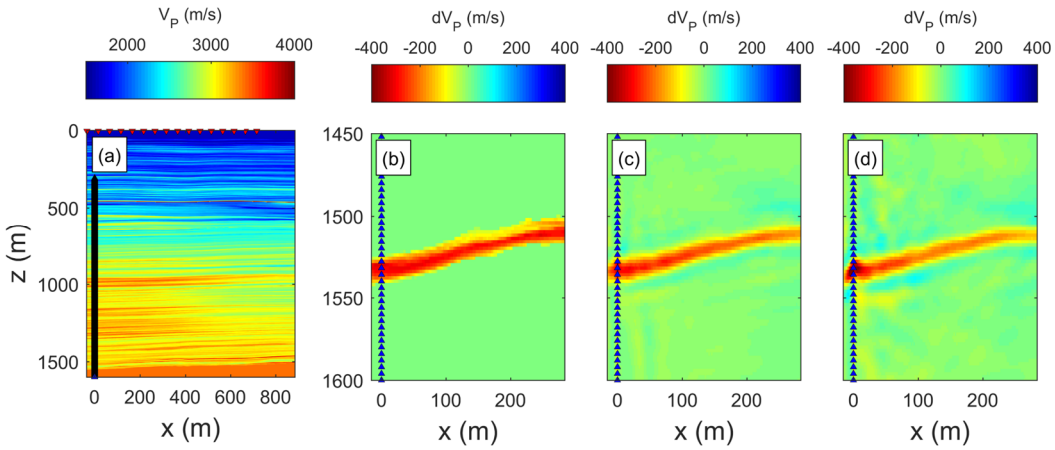

Figure 5.3. Monitor V_P model (a), true V_P difference (b), V_P difference obtained by FWI of 16 sources (c), V_P difference obtained by FWI of 2 permanent sources (d). Maximum frequency is 130 Hz.

However, in this case, the amplitude of the inverted V_P difference is lower than the true V_P changes. This is due to the small thickness of the layer, in which the changes occur. First, the amplitude of the anomaly is not recovered because of the limited frequency range. Second, due to small thickness of the layer, there is a crosstalk between V_P and ρ for high wavenumbers (Pan et al., 2018). To take into account the crosstalk, one can either convert the inverted changes of V_P and ρ into changes in seismic impedance I_P (Figure 5.4), or conduct the inversion with impedance parameterization from the outset.

Overall, this study shows that it is possible to conduct permanent monitoring of injected CO_2 using a DAS cable in the injection well and a small number of permanently installed sources. Different time-lapse inversion strategies, i.e. double-difference and target-oriented inversion, facilitate the reconstruction of time-lapse changes in the subsurface.

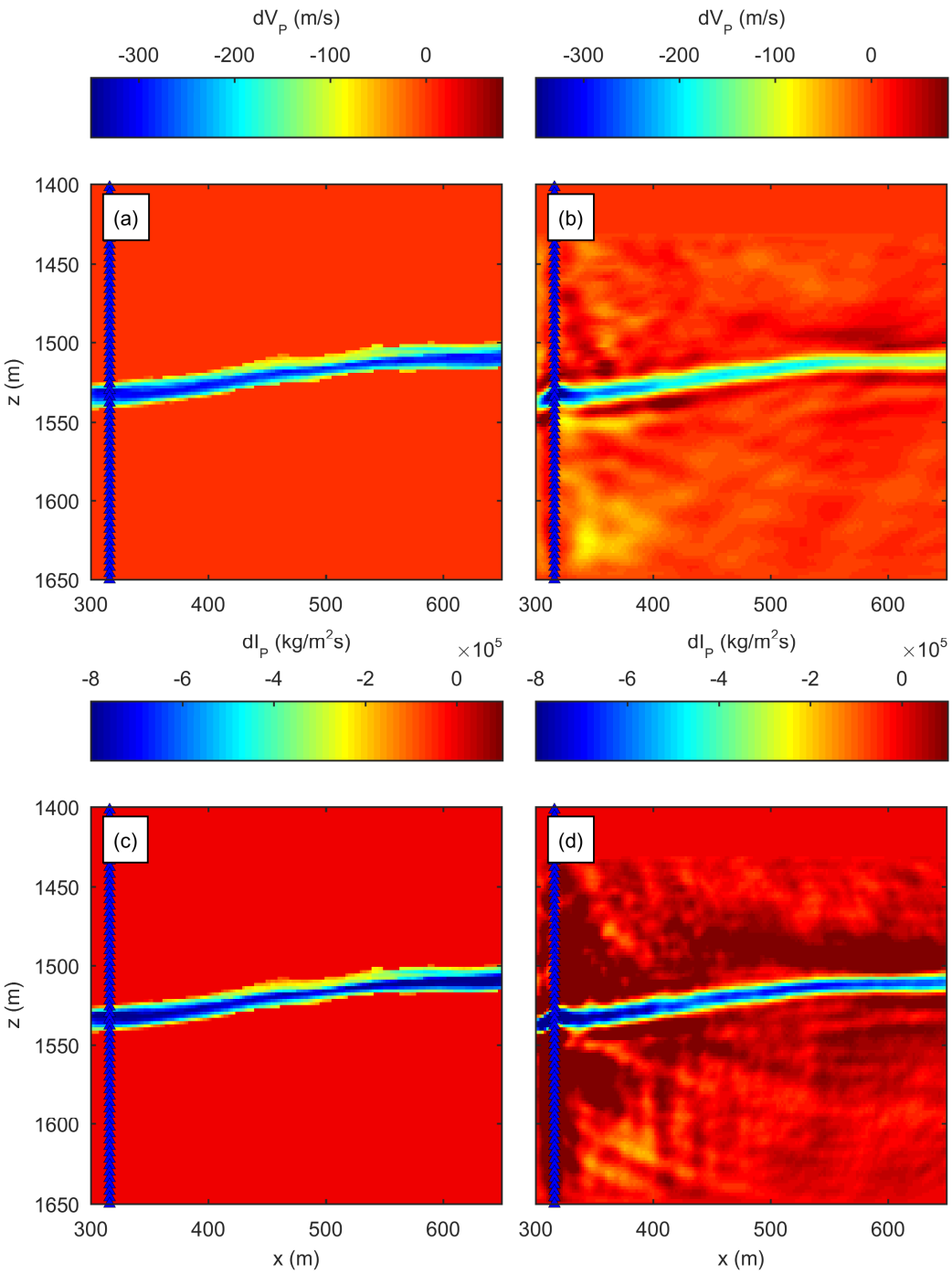

Figure 5.4. Differences in V_P (a-b) and I_P: true (a,c) and inverted (b,d).

Conclusions

This study proposes a FWI workflow and a preprocessing sequence for FWI of VSP data. It shows that FWI of offset VSP datasets is a suitable tool for seismic monitoring. FWI applied to offset VSP provides quantitative estimates of time-lapse changes in P-wave velocity introduced by the CO_2 injection. FWI applications to field data prove that this technique is applicable to real-life monitoring scenarios. Comparison of FWI results for different offsets provides new information about the geometry of the CO_2 plume injected during Stage 2C of the Otway project.

I also investigate the topic of applying FWI to the data obtained with DAS sensors. The results of the conducted studies show that VSP data obtained with DAS systems can be transformed into seismic gathers of particle velocity along the cable. An algorithm for such a transformation is presented. The main limitation of the presented algorithm is the inability to reconstruct the waves with near-infinite apparent velocity, which is a consequence of low sensitivity of DAS to such waves. Despite this limitation, the quality of the conversion makes it possible to conduct FWI of the transformed data to determine the properties of the medium.

Using DAS in conjunction with permanent sources allows the creation of a permanent monitoring system. Tests on synthetic data show that, with the help of such a system, an assessment of time-lapse changes in the properties of the subsurface associated with the injection of CO_2 can be made.

I demonstrate using synthetic datasets that the results of time-lapse inversion can be further improved by constrained optimization methods. Using the sign of change of the properties of the subsurface as a priori information allows one to specify the upper and lower bounds of the inverted properties. With a synthetic data example, I show that the proposed strategy makes it possible to more reliably estimate the changes.

Acknowledgments

I would like to thank:

- my supervisors from Curtin University: Andrej Bóna, Roman Pevzner, Stanislav Glubokovskikh and Vladimir Puzyrev and my supervisor from Lomonosov Moscow State University Mikhail Vladov for their supervision, support and productive discussions.
- Maxim Lebedev, Boris Gurevich and Mikhail Tokarev for the organization of the joint PhD program between Curtin University and Lomonosov Moscow State University.
- Co-authors Konstantin Tertyshnikov and Julia Correa for productive teamwork.
- •Academic and administrative staff of the Curtin Exploration Geophysics Department, especially, Nichole Sik and Sinem Yavuz.
- Authors of the open-source software IFOS2D and SeisCL.
- My wife, my sister and my parents for their support and patience.

I also would like to thank and acknowledge Curtin University for provision of PhD scholarship and CO2CRC for the support of my research project.

References

ASNAASHARI, A., BROSSIER, R., GARAMBOIS, S., AUDEBERT, F., THORE, P. & VIRIEUX, J. 2015. Time-lapse seismic imaging using regularized full-waveform inversion with a prior model: which strategy? *Geophysical Prospecting,* 63**,** 78-98.

BUNKS, C., SALECK, F. M., ZALESKI, S. & CHAVENT, G. 1995. Multiscale seismic waveform inversion. *Geophysics,* 60**,** 1457-1473.

BYRD, R. H., LU, P., NOCEDAL, J. & ZHU, C. 1995. A limited memory algorithm for bound constrained optimization. *SIAM Journal on Scientific Computing,* 16**,** 1190-1208.

CASPARI, E., PEVZNER, R., GUREVICH, B., DANCE, T., ENNIS-KING, J., CINAR, Y. & LEBEDEV, M. 2015. Feasibility of CO_2 plume detection using 4D seismic: CO2CRC Otway Project case study — Part 1: Rock-physics modeling. *Geophysics,* 80**,** B95-B104.

CHARARA, M., BARNES, C. & TARANTOLA, A. 1996. The state of affairs in inversion of seismic data: An OVSP example. *66th Annual International Meeting.* SEG.

CORREA, J., EGOROV, A., TERTYSHNIKOV, K., BONA, A., PEVZNER, R., DEAN, T., FREIFELD, B. & MARSHALL, S. 2017. Analysis of signal to noise and directivity characteristics of DAS VSP at near and far offsets — A CO2CRC Otway Project data example. *The Leading Edge,* 36**,** 994a1-994a7.

DALEY, T., MAYER, L., PETERSON, J. E., MAJER, E. L. & HOVERSTEN, G. M. 2008. Time-lapse crosswell seismic and VSP monitoring of injected CO_2 in a brine aquifer. *Environmental geology* 54**,** 1657-1665

DENLI, H. & HUANG, L. 2009. Double-difference elastic waveform tomography in the time domain. *79th SEG Annual International Meeting.* SEG.

DILLON, P. B. 1990. A comparison bewteen Kirchhoff and GRT migration on VSP data. *Geophysical Prospecting,* 38**,** 757-777.

DOU, S., WOOD, T., AJO-FRANKLIN, J., ROBERTSON, M., DALEY, T., FREIFELD, B., PEVZNER, R. & GUREVICH, B. 2017. Surface orbital vibrator for permanent seismic monitoring: A signal contents and repeatability appraisal. *87th Annual International Meeting.* SEG.

EGOROV, A., BONA, A., PEVZNER, R., GLUBOKOVSKIKH, S. & PUZYREV, V. 2018a. A Feasibility Study of Time-Lapse FWI on DAS VSP Data Acquired with Permanent Sources. *80th EAGE Conference and Exhibition.* EAGE.

EGOROV, A., BONA, A., PEVZNER, R., GLUBOKOVSKIKH, S. & TERTYSHNIKOV, K. 2018b. Application of time-lapse full waveform inversion of vertical seismic profile data for the identification of changes introduced by CO2 sequestration. *ASEG Extended Abstracts,* 2018**,** 1-5.

EGOROV, A., CORREA, J., BÓNA, A., PEVZNER, R., TERTYSHNIKOV, K., GLUBOKOVSKIKH, S., PUZYREV, V. & GUREVICH, B. 2018c. Elastic full-waveform inversion of vertical seismic profile data acquired with distributed acoustic sensors. *Geophysics,* 83**,** R273-R281.

EGOROV, A., PEVZNER, R., BÓNA, A., GLUBOKOVSKIKH, S., PUZYREV, V., TERTYSHNIKOV, K. & GUREVICH, B. 2017. Time-lapse full waveform inversion of vertical seismic profile data: Workflow and application to the CO2CRC Otway project. *Geophysical Research Letters,* 44**,** 7211-7218.

FESSENDEN, R. A. 1917. *Method and apparatus for locating ore bodies* US patent application.

GALPERIN, E. I. & WHITE, J. E. 1974. *Vertical seismic profiling,* Tulsa, Okla., Society of Exploration Geophysicists.

GLUBOKOVSKIKH, S., PEVZNER, R., DANCE, T., CASPARI, E., POPIK, D., SHULAKOVA, V. & GUREVICH, B. 2016. Seismic monitoring of CO_2 geosequestration: CO2CRC Otway case study using full 4D FDTD approach. *International Journal of Greenhouse Gas Control,* 49**,** 201-216.

HATTON, L., MAKIN, J. & WORTHINGTON, M. H. 1986. *Seismic data processing: theory and practice* Oxford, UK, Blackwell Scientific.

JENKINS, C., MARSHALL, S., DANCE, T., ENNIS-KING, J., GLUBOKOVSKIKH, S., GUREVICH, B., LA FORCE, T., PATERSON, L., PEVZNER, R., TENTHOREY, E. & WATSON, M. 2017. Validating Subsurface Monitoring as an Alternative Option to Surface M&V - The CO2CRC's Otway Stage 3 Injection. *Energy Procedia,* 114**,** 3374-3384.

KASAHARA, J., ITO, S., FUJIWARA, T., HASADA, Y., TSURUGA, K., IKUTA, R., FUJII, N., YAMAOKA, K., ITO, K. & NISHIGAMI, K. Y. 2013. Real Time Imaging of CO2 Storage Zone by Very Accurate- stable-long Term Seismic Source. *Energy Procedia,* 37**,** 4085-4092.

KÖHN, D. 2011. *Time domain 2D elastic full waveform tomography.* Ph. D. Thesis, Christian-Albrechts-Universität zu Kiel.

KÖHN, D., DE NIL, D., KURZMANN, A., PRZEBINDOWSKA, A. & BOHLEN, T. 2012. On the influence of model parametrization in elastic full waveform tomography. *Geophysical Journal International,* 191**,** 325-345.

LEANEY, W. S., SAYERS, C. M. & MILLER, D. E. 1999. Analysis of multiazimuthal VSP data for anisotropy and AVO. *Geophysics,* 64**,** 1172-1180.

LEVIN, F. & LYNN, R. 1958. Deep-hole geophone studies. *Geophysics,* 23**,** 639-664.

LIANG, L., LI, M., RUFINO, R., ABUBAKAR, A., NUTT, L., MENKITI, H., DUMMONG, S. & TØNDEL, R. 2013. Application of frequency-domain full-waveform inversion for time-lapse 3D VSP data interpretation. *83rd Annual International Meeting.* SEG.

MAHARRAMOV, M., BIONDI, B. L. & MEADOWS, M. A. 2016. Time-lapse inverse theory with applications. *Geophysics,* 81**,** R485-R501.

MATEEVA, A., LOPEZ, J., POTTERS, H., MESTAYER, J., COX, B., KIYASHCHENKO, D., WILLS, P., GRANDI, S., HORNMAN, K., KUVSHINOV, B., BERLANG, W., YANG, Z. & DETOMO, R. 2014. Distributed acoustic sensing for reservoir monitoring with vertical seismic profiling. *Geophysical Prospecting,* 62**,** 679-692.

NEKLYUDOV, D., SILVESTROV, I. & TCHEVERDA, V. 2013. How Important Are Low Time Frequencies for Offset VSP Full Waveform Inversion? *75th EAGE Conference & Exhibition incorporating SPE EUROPEC.* EAGE.

OWUSU, J. C., PODGORNOVA, O., CHARARA, M., LEANEY, S., CAMPBELL, A., ALI, S., BORODIN, I., NUTT, L. & MENKITI, H. 2016. Anisotropic elastic full-waveform inversion of walkaway vertical seismic profiling data from the Arabian Gulf. *Geophysical Prospecting,* 64**,** 38-53.

PAN, W., INNANEN, K. A. & GENG, Y. 2018. Elastic full-waveform inversion and parametrization analysis applied to walk-away vertical seismic profile data for unconventional (heavy oil) reservoir characterization. *Geophysical Journal International,* 213**,** 1934-1968.

PARKER, T., SHATALIN, S. & FARHADIROUSHAN, M. 2014. Distributed Acoustic Sensing–a new tool for seismic applications. *First Break,* 32**,** 61-69.

PICA, A., DIET, J. P. & TARANTOLA, A. 1990. Nonlinear inversion of seismic reflection data in a laterally invariant medium. *Geophysics,* 55**,** 284-292.

PLESSIX, R. E. 2006. A review of the adjoint-state method for computing the gradient of a functional with geophysical applications. *Geophysical Journal International,* 167**,** 495-503.

PODGORNOVA, O., LEANEY, S., ZEROUG, S. & LIANG, L. 2017. On full-waveform modeling and inversion of fiber-optic VSP data. *87th Annual International Meeting.* SEG.

SHI, Y. & WANG, Y. 2016. Reverse time migration of 3D vertical seismic profile data. *Geophysics,* 81**,** S31-S38.

VIRIEUX, J. & OPERTO, S. 2009. An overview of full-waveform inversion in exploration geophysics. *Geophysics,* 74**,** WCC1-WCC26.

YANG, D., MALCOLM, A., FEHLER, M. & HUANG, L. 2014. Time-lapse walkaway vertical seismic profile monitoring for CO2 injection at the SACROC enhanced oil recovery field: A case study. *Geophysics,* 79**,** B51-B61.

Permission Status: **Granted**

Permission type: Republish or display content
Type of use: Thesis/Dissertation
Job Ticket:
Order License Id:

Hide details

Requestor type	Author of requested content
Format	Print, Electronic
Portion	chapter/article
The requesting person/organization	Mr. Anton Egorov
Title or numeric reference of the portion(s)	Elastic full-waveform inversion of vertical seismic profile data acquired with distributed acoustic sensors (whole paper)
Title of the article or chapter the portion is from	Elastic full-waveform inversion of vertical seismic profile data acquired with distributed acoustic sensors
Editor of portion(s)	N/A
Author of portion(s)	A. Egorov et al.

Confirmation Number: 11736594

Citation Information

Order Detail ID: 71405926

Geophysics by Society of Exploration Geophysicists ; American Institute of Physics ; Society of Exploration Geophysicists Reproduced with permission of SOCIETY OF EXPLORATION GEOPHYSICISTS in the format Thesis/Dissertation via Copyright Clearance Center.

Close

To Whom It May Concern

I, *Anton Egorov*, contributed to *conditioning, manipulation, analysis and interpretation of data, as well as to the writing of* the paper/publication entitled "*Time-lapse full waveform inversion of vertical seismic profile data: Workflow and application to the CO2CRC Otway project*", Geophys. Res. Lett., 44, 7211– 7218.

I, as a Co-Author, endorse that this level of contribution by the candidate indicated above is appropriate.

Name of the Co-Author	**Signature**
Roman Pevzner	
Andrej Bona	
Stanislav Glubokovskikh	
Vladimir Puzyrev	
Konstantin Tertyshnikov	
Boris Gurevich	

To Whom It May Concern

I, *Anton Egorov*, contributed to *conditioning, manipulation, analysis and interpretation of data, as well as to the writing of* the paper/publication entitled "*Elastic full-waveform inversion of vertical seismic profile data acquired with distributed acoustic sensors*", GEOPHYSICS, 2018, 83:3, R273-R281.

I, as a Co-Author, endorse that this level of contribution by the candidate indicated above is appropriate.

Name of the Co-Author	**Signature**
Julia Correa	
Andrej Bona	
Roman Pevzner	
Konstantin Tertyshnikov	
Stanislav Glubokovskikh	
Vladimir Puzyrev	
Boris Gurevich	

To Whom It May Concern

I, *Anton Egorov*, contributed to *conditioning, manipulation, analysis and interpretation of data, as well as to the writing of* the paper/publication entitled "*Analysis of signal to noise and directivity characteristics of DAS VSP at near and far offsets — A CO2CRC Otway Project data example*", The Leading Edge, 2017, 36:12, 994a1-994a7.

I, as a Co-Author, endorse that this level of contribution by the candidate indicated above is appropriate.

Name of the Co-Author	**Signature**
Julia Correa	
Konstantin Tertyshnikov	
Andrej Bona	
Roman Pevzner	
Tim Dean	
Barry Freifeld	
Steve Marshall	